Fluorescence concerns in high energy x-ray yield scaling and imaging studies

George A. Kyrala[a] and Jonathan B. Workman
Los Alamos National Laboratory, Box 1663, Mail Stop E-526, Los Alamos, New Mexico 87545

(Presented on 20 June 2000)

X rays at high photon energies are needed to backlight and image large objects of high opacity on large lasers, such as the National Ignition Facility, or large pulsed power facilities, such as ATLAS. Attenuators and filters are usually used to bring the signals to scale and to filter the x rays from un-needed low energy components. As the x-ray energy increases, the secondary effect of the interactions of the x rays with the filter or attenuator material must be addressed. This is especially true when one considers using the very high energy x rays from the hot electrons generated during the interaction of intense lasers with high Z materials. We will show how these concerns can be quantified and reduced in at least one case; an experiment on the OMEGA laser facility, designed to investigate the scaling of absolute x-ray yield and conversion efficiency with laser energy and power. This investigation is part of the study to determine the feasibility of high-energy backlighters using Ge emission near 10.3 keV. We will also show how these results apply to imaging at larger x-ray energies. [DOI: 10.1063/1.1318252]

I. INTRODUCTION

Filters have been used for many years in the inertial confinement fusion (ICF) and pulsed power program to measure the emitted spectrum from a device.[1–4] They are used as simple elements that select or reject some part of an incident x-ray spectrum. Tabular x-ray attenuation coefficients[5–8] are used to calculate the transmission of such filters. Such simple calculations have been implemented in at least two free software packages[9,10] showing the transmission of the x-ray lines at each wavelength but do not show what happens to the part that was absorbed. For many systems that measure the absolute energy of the incident radiation or that measure the transmitted spectrum, this neglect may generate a significant distortion of the expected or perceived spectrum. Few treatments of this problem have been shown in the literature, especially for the case of x-ray fluorescence from the illuminated side of a filter.[11–13] We did not find a single reference that deals with the modification to the transmitted x-ray spectrum, but we found one reference that dealt with the backscatter spectrum.[14] However, as interest increases in radiographing and backlighting thicker objects that require higher x-ray energies these effects cannot be neglected and should be included in the analysis. In this article we introduce the relevant concepts in a manner similar to that of the reflected x rays, and apply that to a real situation. We also discuss how to reduce these effects to manageable proportions.

II. FLUORESCENCE

X rays can be attenuated either by scattering, by pair production, or by the photoelectric effect. When they are attenuated by the photoelectric effect, a vacancy occurs in any of the shells whose ionization energy is lower than that of the x-ray line of interest. The vacancies may be filled by either an electron from a separate shell, generating a fluorescent x ray, or by Auger emission of another electron without x-ray generation.[15,16] Generally it has been found that the fluorescence efficiency increases with the nuclear charge of the target element and decreases with the ionization energy of the shell of interest. Multiple ionization and cascade effects may occur, and are usually included in the measured fluorescence efficiency.

In order to get a feeling for the magnitude of the problem, we may write the equations in a manner similar to Ref. 13. However, for the purposes of this section, we will; look only along the axis, neglect the angular effects, assume that the incident x rays are collimated and have an extent much wider than the thickness of the foil, and assume that the filter is made of a simple single element. The incident spectral photon flux density, $I_\lambda(x)=\partial I/\partial\lambda$ is measured at a depth x, in units of photons per unit bandwidth interval per unit area, attenuated to a value $I_\lambda(0)d\lambda e^{-\mu\rho x}$, where $\mu_\lambda=\mu_\lambda^s+\mu_\lambda^p+\mu_\lambda^\pi$ is the total linear mass absorption coefficient at a wavelength λ, the sum of scattering, photoelectric, and pair production coefficients, respectively, and where ρ is the density of the foil.

The number of photons depleted from the beam in a thickness dx at depth x is then $I_\lambda(0)d\lambda e^{-\mu\rho x}\mu_\lambda\rho dx$. But of those only a fraction, absorbed by the photoelectric effect, gives a hole, and only if the incident photon energy is greater than the binding energy of that shell: No. holes $=I_\lambda(0)d\lambda e^{-\mu\rho x}\mu_\lambda^p\rho dx$. Of those holes a fraction produces a K shell vacancy: No. K shell Vacancies=No. holes*$(r_k-1)/r_k$. Where r_k is the jump factor in the photoelectric absorption coefficient at the K edge. The rest are absorbed in higher shells.

Of those holes in the K shell, only a fraction ω_k is filled by K-alpha and K-beta line fluorescence.[15,16] For illustrative

[a]Electronic mail: kyrala@lanl.gov

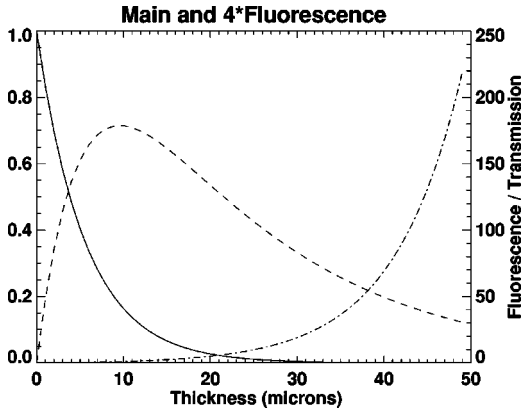

FIG. 1. The growth and decay of the Fe *K*-alpha line, the Zn He-alpha line and the ratio of photons in the Fe and Zn lines, continuous dashed and dot dash, respectively, for different depths into the iron filter.

purposes of this section we group the two lines into a single *K* line. The fluorescent radiation is emitted uniformly in every direction and a fraction $c=d\Omega/4\pi$ of the *K* radiation propagates in the forward direction. The *K* lines propagate through the rest of the filter, of thickness *h*, emerging with a photon flux from a unit spectral cut of:

$$F_k(h)d\lambda = \int_0^h cI_\lambda(0)d\lambda e^{\mu\rho x}\mu_\lambda^p \rho dx\left[\frac{r_k-1}{r_k}\right] \times \omega_k e^{-\mu_k\rho(h-x)},$$

$$F_k(h)d\lambda = \left[\frac{r_k-1}{r_k}\right][c\omega_k]\left[\frac{\mu_\lambda^p}{\mu_\lambda-\mu_k}\right] \times [1-e^{-\rho h(\mu_\lambda-\mu_k)}]I_\lambda(0)d\lambda e^{-\mu_k\rho h},$$

where μ_k is the total absorption coefficient at the wavelength of the fluorescent *K* lines. Contrast this with normally calculated fluorescence in the backward direction[14]

$$B_k(h)d\lambda = \left[\frac{r_k-1}{r_k}\right][c\omega_k]\left[\frac{\mu_\lambda^p}{\mu_\lambda-\mu_k}\right] \times [1-e^{-\rho h(\mu_\lambda+\mu_k)}]I_\lambda(0)d\lambda.$$

The transmission of the filter at the incident radiation wavelength is given by $e^{-\rho h\mu_\lambda}I_\lambda(0)d\lambda$. There is a peak in the forward yield at a depth $H=\log_e(\mu_\lambda^p/\mu_\lambda)/[(\mu_k-\mu_\lambda)\rho]$.

In contrast, the yield in the backward direction saturates with foil thickness and does not show a peak. If we take as an example the transmission of the zinc He_α line in an iron filter, the peak occurs at a thickness $H=9.5\,\mu$m with a peak fluorescent fraction of 0.18. In other words, 18% of the incident photons are transmitted and 9% are converted into iron *K*-alpha lines that emerge from the filter along the initial propagation direction of incident x rays (Fig. 1).

Of course the emitted fluorescence disperses into all directions, while the transmitted flux at the incident wave length remains as a noncollimated beam. Interestingly, in Fig. 1, the ratio of the fluorescent radiation to the emergent radiation at the initial frequency is a monotonically increasing function of the foil thickness!

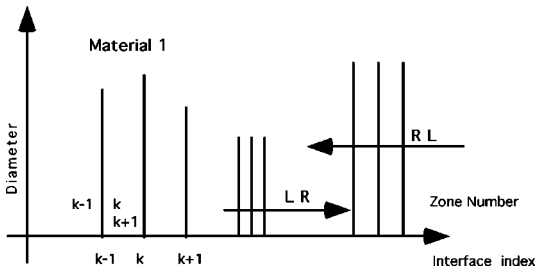

FIG. 2. Schematic diagram of the zoning used.

III. EXACT CALCULATIONS

The simple calculation in the previous section shows that there may be a problem when designing filter sets indiscriminately. In a real system there are other effects that should be included, such as secondary, tertiary and higher order fluorescence, as well as scattering. In a multilayer system, backward going fluorescence may also excite other lines that may effect the forward going flux. Two-dimensional effects are important as well but, as shown in Ref. 12, those effects are equivalent to secondary fluorescence and although difficult to calculate the effect is second order if the fluorescence efficiency is not too great, and if the detector is far from the fluor. In Sec. IV we will describe the method used to evaluate a real system using a more complete description of the problem.

We assume that we have a set of filters each made of unique elements, having any cross-sectional areas, and present in any location between the source and the detector. The problem may then be reduced to calculating a left-to-right going x-ray flux, along the incident x-ray direction, and a right-to-left going flux antiparallel to the incident direction. Each material is subdivided into thin layers called zones, each thinner than the mean free path of the radiation in the foil (Fig. 2). The x-ray spectrum is subdivided into very narrow zones, typically an eV wide. For a given zone the right going photon flux $LR(k,n)$ is a function of the position index *k* and the energy index *n*. The absorption coefficient for that zone $\mu(n,b)$ is a function of the energy index *n*, and the material index *b* (usually *b* is the *z* of the material). Then we can write the recursion formulas: $LR(k,n)=LR(k-1,n)*m(n,b)$ and $RL(k,n)=RL(k+1,n)*m(n,b)$. Where the index *k* refers to the right surface of the zone in region *k* (see Fig. 2) and $m(n,b)=\exp\{-\rho(k)t(k)\mu[b(k),n]\}$ is the attenuation of the zone *k* of thickness $t(k)$, density $\rho(k)$ at the energy with index *n* for material *b* with index $b(k)$.

When the energy of the x ray in a given zone exceeds the absorption energy of an edge, in that material, then we calculate a number of holes from the energy absorbed above the edge into the shell, from both right and left going fluxes

$$H(k)=\sum_{n>n_k}[\{LR(k-1,n)-LR(k,n)\} +\{RL(k,n)-RL(k-1,n)\}]\left[\frac{r_k-1}{r_k}\right],$$

where we added the contributions from the two propagation directions.

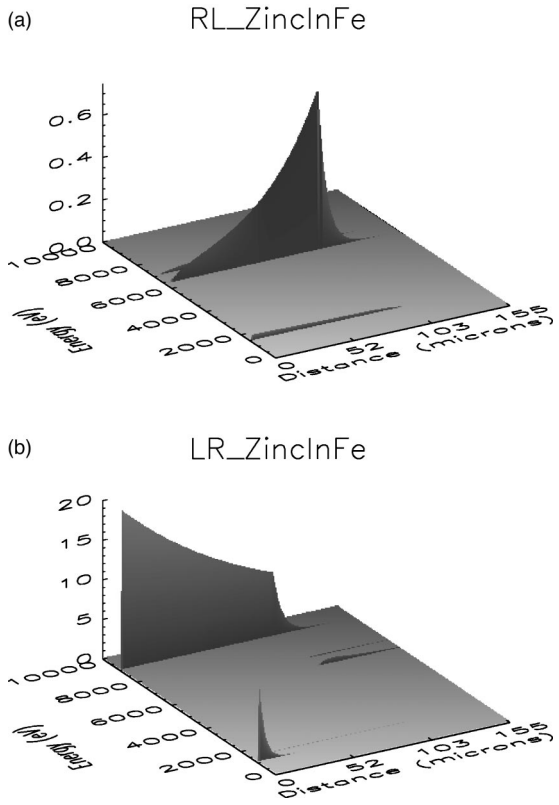

FIG. 3. (a) The left-to-right going spectrum as a function of depth. Note the break at the Al–iron interface, and the growth of the Fe *K* lines. (b) The right-to-left going spectrum as a function of depth. The *K*-alpha photons are generated in the iron but decay into the aluminum. The low energy fluorescence continue to grow in the backward direction.

The output fluorescent flux is then divided into forward and backward components apportioned to each fluorescent line using the appropriate fluorescent efficiency for that line, and the solid angle between the two zone boundaries

$$LR(k,n_{ka}) = LR(k,n_{ka}) + H(k)\omega_k\left[\frac{r_k-1}{r_k}\right]\Omega_{k,k+1}\left[\frac{n_{ka}}{n_{k\alpha}+n_{k\beta}}\right]$$

with a similar expression for each line and for the *RL* spectral flux density.

IV. EXAMPLE

As an example, to show the effect of the filter composition on the measured result, we simulated a laser-plasma generated spectrum incident on an aluminum filter that is backed off from an iron filter. The filters (100 μm of Al, followed by a 400 μm gap, then 50 μm of iron, and finally a 2 μm of Be) were placed in front of a detector. The incident spectrum consisted of two x-ray lines at 1056 and 8999 eV, and a bremstrahlung background of 200 keV temperature, but with a small amplitude. The Fe is used to attenuate the He-like Zn line by a factor of 10 000 so as not to saturate the detector. The transmitted and reflected spectral fluxes are shown in Figs. 3(a) and 3(b), respectively, as a function of depth. The output, Fig. 4, is found to have the expected fluorescence from the iron *K* lines, but with a larger transmission for the fluorescent line relative to the input line.

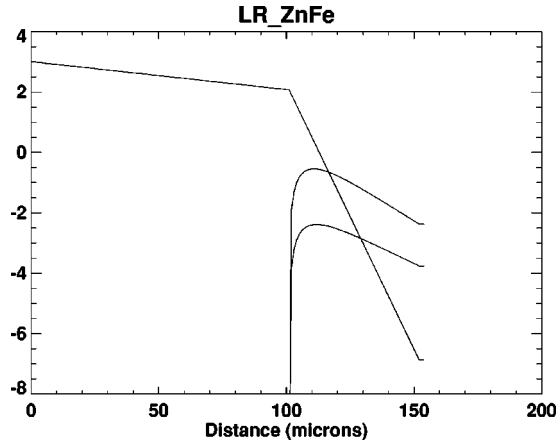

FIG. 4. The attenuation of the helium-like line of Zn and the relative growth of the *K*-alpha and *K*-beta lines of iron as a function of foil depth, continuous, dash, and dot-dash, respectively. At the exit, the iron contribution exceeds the transmitted incident zinc flux.

Thus this design would not have served the purposes that we would have expected without regard to the fluorescence. In contrast we would have accomplished our purpose with 1 mm of Al to perform the same attenuation, but without a fluorescent spectrum.

An alternative solution would have been to put the detector a significant distance from the source. In this case the incident flux at the 8999 keV would not have been changed by solid angle, but the fluorescent radiation would have been. Assuming the same area as in the example, the distance would have had to be more than 25 cm for the fluorescent radiation flux to be 10% of the desired line, however the transmitted band below the *K* edge of iron would still contribute significantly to the measured signal. In contrast with previous work where the filters were *conveniently* put next to the film or the gated instruments, this analysis led us to use a new modified *nose cone* that contained the filters.

V. DISCUSSION

The above examples led us to some fundamental conclusions relative to the use of filters; we found that to be on the safe side, only low-*z* material should be used for attenuation. The most convenient element is aluminum. Aluminum fluoresces little and only at low x-ray energies that can be easily attenuated by Be or C shields. Since it is also a low *Z* material, Al scatters the radiation with low efficiency; the coherent scattering cross section is $<10\%$ of the photoelectric cross section below 20 keV. We also found that to attenuate a single He-like line, it is better to use the same material that originates the line to perform the attenuation. Since for most material with $z>18$ the helium like line are below the *K* edge of the material, their absorption cannot produce a vacancy and hence cannot produce *K*-shell fluorescence. The *L* and *M* shell fluorescence is not efficient and would be easily filtered.

We also show that the fluorescence technique may be used as a very powerful measuring tool for the detection of hot electrons. Filter fluorescence from the front of foils inclined at 45° has been used extensively to measure high

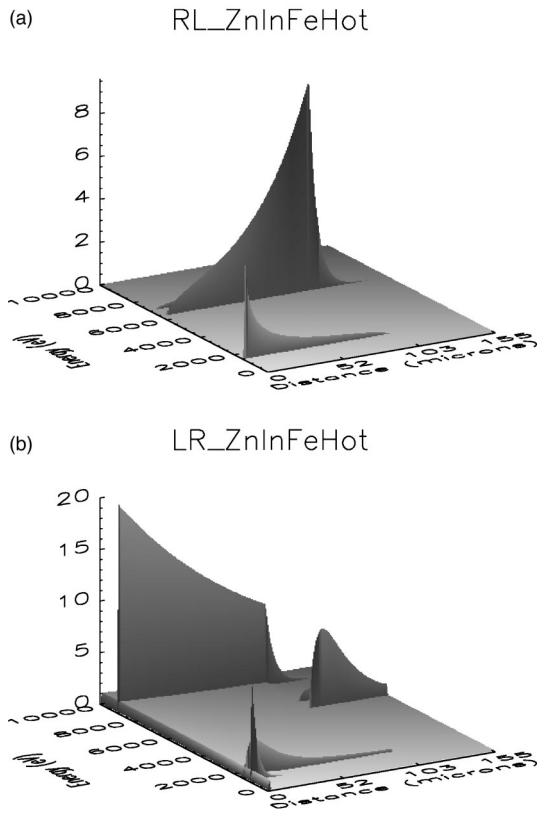

FIG. 5. (a) The left-to-right going spectrum as a function of depth. Note the break at the Al–iron interface, and the growth of the Fe *K* lines. The *K*-alpha line is larger than in Fig. 3, mostly due to the absorption from tail of the bremstrahlung. (b) The right-to-left going spectrum as a function of depth. The *K*-alpha are generated in the iron but decays into the aluminum, but the low energy fluorescence continue to grow in the backward direction.

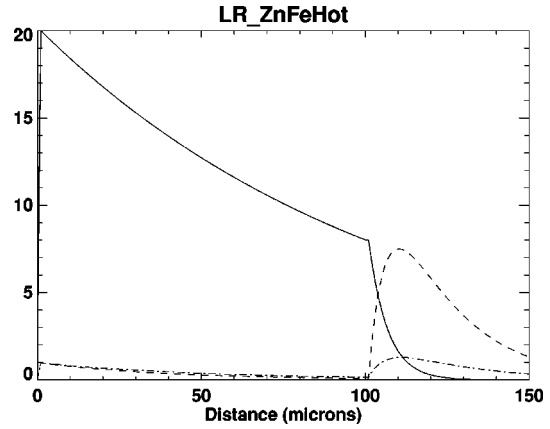

FIG. 6. The attenuation of the helium-like line of Zn and the relative growth of the *K*-alpha and *K*-beta lines of iron as a function of foil depth. At the exit, the iron contribution exceeds the transmitted incident zinc flux by a large margin.

x-ray energy yield, but has not been considered as we mention here, in the forward direction.[17] In Figs. 5 and 6, we repeat the calculation but with a large hot electron contribution, 10 000 times bigger than in Figs. 3 and 4. We chose the example carefully to put the continuum at a level of 3 orders of magnitude below the peak, at the limit of the dynamic range of film. A normal crystal spectrometer would not have seen this contribution easily, and would have been interpreted as a constant background or a level shift. Normally one observes the direct excitation of the *K*-alpha line by electron impact. However, the *K*-alpha radiation is also sensitive to the total number of photons in the spectrum above the *K* edge. By selecting few materials with different *K* edges one may be able to measure the temperature of the spectrum, even when the spectrum is weak and may not be recordable with normal crystal spectrometers. We also note that in measuring the *K*-alpha yield from hot electrons we must ensure that fluorescence from the rampant high-energy photon in the tail of the x-ray spectrum did not contribute significantly to the recorded *K*-alpha signal. The expected spectrum now shows a large contribution solely due to the hot electron bremstrahlung contribution, and not to direct excitation. The output spectrum, Fig. 5(a), is identical to the previous no Bremstrahlung case, Fig. 4(a), but the amplitude is larger. Thus measuring the spectrum is no proof that fluorescence was not a contributing factor, and using different filters is the only method to distinguish between direct excitation and bremstrahlung induced fluorescence.

Finally, we note that fluorescence may contribute to reduce the modulation transfer function (MTF) of the recording systems. If a foil is placed close to the recording plane, it will cast a significant penumbra on the instrument. As in measuring the flux, this may be reduced by putting the filters as far from the recording plane as possible, which would reduce the fluorescence signal, and would make the shadows sharper. Since the signal is purer now, the measured noise in the spectrum would be a true measure of the noise in the system unmodified by the noise due to the secondary fluorescence. This analysis also points out the difficulty of interpreting MTF measurements at high x-ray energy when the modulating substrate may fluoresce.

ACKNOWLEDGMENT

This work was performed under the auspices of the U.S. Department of Energy under Contract No. W-7405 ENG-36.

[1] R. H. Day, P. Lee, E. B. Salomon, and D. J. Nagel, Los Alamos Scientific Laboratory Report No. LA-UR-79-1360 (unpublished).
[2] J. L. Gaines, H. N. Kornblum, and V. M. Slivinsky, Lawrence Livermore Laboratory Report No. UCRL 75987 A, 1974 (unpublished).
[3] C. L. Wang, Rev. Sci. Instrum. **53**, 582 (1982).
[4] H. N. Kornblum and R. L. Kauffman, Rev. Sci. Instrum. **57**, 2179 (1986).
[5] B. L. Henke, P. Lee, T. J. Tanaka, R. L. Shimabukuro, and B. K. Fujikawa, At. Data Nucl. Data Tables **27**, 3 (1982).
[6] B. L. Henke, E. M. Gullikson, and J. C. Davis, At. Data Nucl. Data Tables **54**, 181 (1993).
[7] F. Biggs and R. Lighthill, Sandia Report No. SAND87-0070 (unpublished).
[8] E. Storm and H. I. Israel, Nucl. Data Sect. A **7**, 565 (1970).
[9] G. A. Kyrala, Rev. Sci. Instrum. **63**, 4768 (1992).
[10] See for example http://www-cxro.lbl.gov/optical_constants/
[11] E. Gillam and H. T. Heal, Br. J. Appl. Phys. **3**, 353 (1952).
[12] T. Shirawa and N. Fujino, Jpn. J. Appl. Phys. **5**, 886 (1966).
[13] R. Tertian and F. Claisse, *Principles of Quantitative X-ray Fluorescence Analysis* (Heyden, Philadelphia, 1982).
[14] J. E. Fernandez, X-Ray Spectrom. **21**, 57 (1992).
[15] M. H. Chen and B. Crasemann, At. Data Nucl. Data Tables **24**, 13 (1979).
[16] M. O. Krause, J. Phys. Chem. Ref. Data **8**, 307 (1979).
[17] K. G. Tirsell and H. C. Catron, Lawrence Livermore Laboratory, Report No. UCRL-80314 (1977) (unpublished).